COMPDYN 2013
4th ECCOMAS Thematic Conference on
Computational Methods in Structural Dynamics and Earthquake Engineering
M. Papadrakakis, V. Papadopoulos, V. Plevris (eds.)
Kos Island, Greece, 12–14 June 2013

NONLINEAR VIBRATIONS OF ROTATING 3D TAPERED BEAMS WITH ARBITRARY CROSS SECTIONS

S. Stoykov[1], **S. Margenov**[1]

[1] Institute of Information and Communication Technologies, Bulgarian Academy of Sciences
Acad. G. Bonchev str., bl. 25A, 1113 Sofia, Bulgaria
{stoykov, margenov}@parallel.bas.bg

Keywords: *p*-version finite element method, warping function, acceleration of Coriolis, setting angle, bending-bending coupling.

Abstract. *The geometrically nonlinear vibrations of 3D beams that rotate about a fixed axis are investigated by the p-version finite element method. The beams are considered to be tapered, i.e. with variable thickness along its length, and with arbitrary cross sections. The beam model is based on Timoshenko's theory for bending and Saint-Venant's theory for torsion, i.e. it is assumed that the cross section rotates about the longitudinal axis as a rigid body but may deform in longitudinal direction due to warping and the torsion is not considered to be uniform. The warping function is obtained preliminarily by the finite element method. For the case of tapered beams, the warping and torsional constants, the cross sectional area, the second moment of inertia and all cross sectional properties are expressed as functions of the longitudinal local coordinate. Geometrical nonlinearity is taken into account and derived from Green's strain tensor. Linear elastic and isotropic materials are considered and generalized Hooke's law is used. The rotation is included in the model through the inertia terms, two coordinate systems are considered: one fixed and one rotating about the fixed one. The equation of motion is derived by the principle of virtual work in the rotating coordinate system but the influence of the rotation of the coordinate system on the displacements of the beam is included in the equation of motion. A setting angle and hub radios are considered, and their influence, as well the influence of the speed of rotation, on the natural frequencies is examined. Forced vibrations in time domain are presented for various setting angles.*

1 INTRODUCTION

Rotating beams are used to model and investigate the dynamics of helicopter blades, jet engine turbine blades, robot arms, wind turbine blades, etc. Many studies have been performed for modeling rotating beams about a fixed axis. The linear natural frequencies of beams that rotate with constant speed were investigated by many researchers, for example in [1-5]. Works that consider geometrically nonlinear models of rotating beams may be found, for example [6-8]. In what concerns modern wind turbine blades, most of them are constructed with load carrying box girder inside the blade and shells on the surface of the blade [9]. The purpose of the box girder is to make the blade stronger and stiffer while the shells around the box girder form the aerodynamic shape. Thus, the dynamic behavior of the wind turbine blade might be determined mainly from the load carrying box, even though the shells contribute small bending strength.

In the current work, a model of beams rotating about a fixed axis with constant speed of rotation is presented. A setting angle and a rigid hub are included in the model. The equation of motion is derived in the rotating coordinate system, and the rotation is taken into account by the inertia forces [10]. The beam may vibrate in space, i.e. it may perform longitudinal, torsional and bending deformations, the model is based on Timoshenko's theory for bending and assumes that under torsion, the cross section deforms only in longitudinal direction due to warping [11]. Geometrical type of nonlinearity is considered and the equation of motion is derived by the principle of virtual work.

Thin-walled box beams with linearly varying thickness and width are investigated. First, the derived model is validated by generating a fine mesh of three-dimensional finite elements. Then, the influence of the setting angle and the speed of rotation on the natural frequencies is examined. Forced vibrations of rotating beams due to harmonic forces are presented.

2 MATHEMATICAL MODEL

Tapered beams with linearly varying thickness and arbitrary cross section, in elastic, homogeneous and isotropic materials, that rotate about a fixed axis with constant angular speed are considered. The beam equation of motion is derived in a rotating coordinate system and the rotation of the coordinate system is taken into account into the equation of motion. Two coordinate systems are used for that purpose: the first one (*XYZ*) is fixed in space, it will be denoted with S_0, the second coordinate system (*xyz*) rotates around the *Z* axis of the fixed coordinate system, it will be called "transport coordinate system" and denoted with S_1. A setting angle φ is considered in the model, i.e. angle which inclines the cross section to the plane of rotation, thus the *z* axis of the transport coordinate system is inclined on angle φ with respect to *Z* axis of the fixed coordinate system, and the *x* axis of the transport coordinate system, which presents the longitudinal direction the beam remains in the plane of rotations, i.e. *XY* (Figure 1). The beam is assumed to be rigidly mounted on hub with radios *R*. The centers of both coordinate systems coincide. The transport coordinate system rotates with a constant speed, $\vartheta(t)$ rad denotes its rotation at time *t*, then $\dot{\vartheta}(t)$ is the speed of rotation (rad/s), or angular velocity. The beam equation of motion is derived with one *p* element and improving the accuracy of the results is achieved by increasing the number of the shape functions.

2.1 Beam equation of motion in transport coordinate system

The displacements of the beam are expressed in the transport coordinate system S_1, assuming Timoshenko's theory for bending [12] and Saint-Venant's theory for torsion [13], including deformation in longitudinal direction due to warping:

$$u(x,y,z,t) = u_0(x,t) - y\,\phi_z(x,t) + z\,\phi_y(x,t) + \psi(y,z)\,\frac{\partial\theta_x}{\partial x}(x,t)$$
$$v(x,y,z,t) = v_0(x,t) + y\cos\big(\theta_x(x,t)\big) - y - z\sin\big(\theta_x(x,t)\big) \quad (1)$$
$$w(x,y,z,t) = w_0(x,t) + y\sin\big(\theta_x(x,t)\big) + z\cos\big(\theta_x(x,t)\big) - z$$

where u presents the longitudinal displacement, v and w present the transverse displacements in y and z directions, the subscript 0 denotes the displacements on the reference line, θ_x is the rotation of the cross section about the longitudinal axis x, ϕ_y and ϕ_z denote rotations of the cross section about axes y and z, respectively and $\psi(y,z)$ is the warping function.

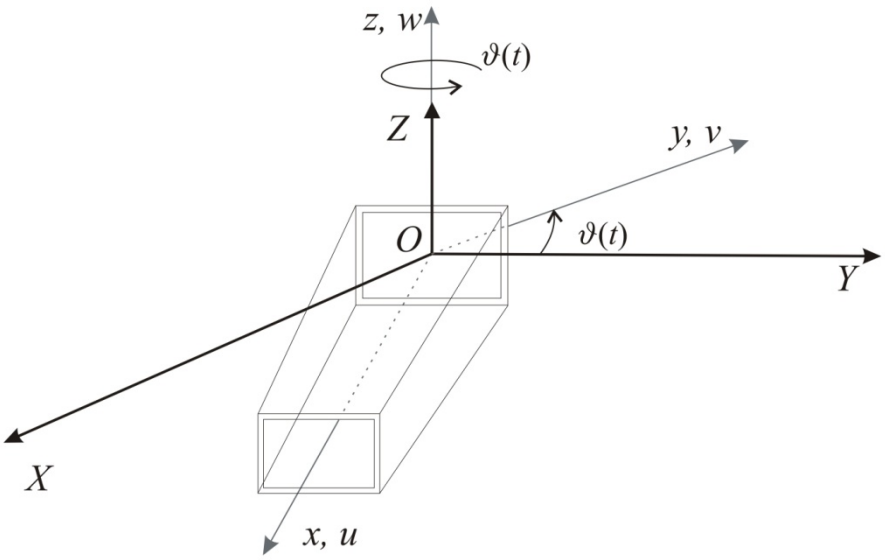

Figure 1. Axes and displacements of rotating beam model.

The equation of motion is derived by the principle of virtual work and the rotation of the beam is considered in the inertia forces by using the absolute acceleration, i.e. the acceleration with respect to the fixed coordinate system [14]. The equation of motion is derived in the rotating coordinate systems, thus the absolute acceleration of an arbitrary point P(x,y,z) from the beam is written at that coordinate system:

$$\boldsymbol{a}_{P_{S_0}} = \boldsymbol{a}_{P_{S_1}} + \boldsymbol{\alpha}_{10} \times \boldsymbol{r} + \boldsymbol{\omega}_{10} \times (\boldsymbol{\omega}_{10} \times \boldsymbol{r}) + 2\,\boldsymbol{\omega}_{10} \times \boldsymbol{v}_{P_{S_1}} \quad (2)$$

where $\boldsymbol{a}_{P_{S_0}}$ is the absolute acceleration of point P, i.e. the acceleration of point P with respect to S_0, $\boldsymbol{a}_{P_{S_1}}$ is the relative acceleration of point P, i.e. the acceleration of point P with respect to S_1, given in (3), $\boldsymbol{v}_{P_{S_1}}$ is the relative velocity of point P, i.e. the velocity of point P with respect to S_1, given in (4), $\boldsymbol{\omega}_{10}$ is the angular velocity of the transport coordinate system (5), $\boldsymbol{\alpha}_{10}$ is the angular acceleration vector of the transport coordinate system which is assumed to be zero, since beams rotating with constant speed are analyzed, and $\boldsymbol{r}$ is the position vector of point P with respect to the origin of S_1 (6). Furthermore, $\boldsymbol{\omega}_{10} \times (\boldsymbol{\omega}_{10} \times \boldsymbol{r})$ is the transport acceleration, and $2\,\boldsymbol{\omega}_{10} \times \boldsymbol{v}_{P_{S_1}}$ is the acceleration of Coriolis.

$$\boldsymbol{a}_{P_{S_1}} = \begin{Bmatrix} \ddot{u}_0 - y\,\ddot{\phi}_z + z\,\ddot{\phi}_y + \psi\frac{\partial\ddot{\theta}_x}{\partial x} \\ \ddot{v}_0 - y\cos(\theta_x)(\dot{\theta}_x)^2 - y\sin(\theta_x)\,\ddot{\theta}_x + z\sin(\theta_x)\big(\dot{\theta}_x\big)^2 - z\cos(\theta_x)\ddot{\theta}_x \\ \ddot{w}_0 - y\sin(\theta_x)(\dot{\theta}_x)^2 + y\cos(\theta_x)\,\ddot{\theta}_x - z\cos(\theta_x)\big(\dot{\theta}_x\big)^2 - z\sin(\theta_x)\ddot{\theta}_x \end{Bmatrix} \quad (3)$$

$$\boldsymbol{v}_{\boldsymbol{P}_{\boldsymbol{S}_1}} = \begin{Bmatrix} \dot{u}_0 - y\,\dot{\phi}_z + z\,\dot{\phi}_y + \psi\dfrac{\partial \dot{\theta}_x}{\partial x} \\ \dot{v}_0 - y\sin(\theta_x)\,\dot{\theta}_x - z\cos(\theta_x)\,\dot{\theta}_x \\ \dot{w}_0 + y\cos(\theta_x)\,\dot{\theta}_x - z\sin(\theta_x)\,\dot{\theta}_x \end{Bmatrix} \tag{4}$$

$$\boldsymbol{\omega}_{\mathbf{10}} = \begin{Bmatrix} 0 \\ \dot{\vartheta}\sin\varphi \\ \dot{\vartheta}\cos\varphi \end{Bmatrix} \tag{5}$$

$$\boldsymbol{r} = \begin{Bmatrix} R + x + u_0 - y\,\phi_z + z\,\phi_y + \psi\dfrac{\partial \theta_x}{\partial x} \\ y + v_0 + y\cos(\theta_x) - y - z\sin(\theta_x) \\ z + w_0 + y\sin(\theta_x) + z\cos(\theta_x) - z \end{Bmatrix} \tag{6}$$

where R is the hub radios.

The absolute acceleration can be written as

$$\ddot{\mathbf{d}} = \begin{Bmatrix} \ddot{u} \\ \ddot{v} \\ \ddot{w} \end{Bmatrix} = \begin{Bmatrix} \ddot{u}_R + \ddot{u}_T + \ddot{u}_C \\ \ddot{v}_R + \ddot{v}_T + \ddot{v}_C \\ \ddot{w}_R + \ddot{w}_T + \ddot{w}_C \end{Bmatrix} \tag{7}$$

where the subscripts $_R$, $_T$ and $_C$ denote relative, transport and acceleration of Coriolis, respectively, given by:

$$\begin{aligned} \ddot{u}_R &= \ddot{u}_0 - y\;\ddot{\phi}_z + z\,\ddot{\phi}_y + \psi\frac{\partial \ddot{\theta}_x}{\partial x} \\ \ddot{v}_R &= \ddot{v}_0 - y\;\cos(\theta_x)(\dot{\theta}_x)^2 - y\;\sin(\theta_x)\,\ddot{\theta}_x + z\sin(\theta_x)\left(\dot{\theta}_x\right)^2 - z\cos(\theta_x)\ddot{\theta}_x \\ \ddot{w}_R &= \ddot{w}_0 - y\;\sin(\theta_x)\left(\dot{\theta}_x\right)^2 + y\;\cos(\theta_x)\,\ddot{\theta}_x - z\cos(\theta_x)\left(\dot{\theta}_x\right)^2 - z\sin(\theta_x)\ddot{\theta}_x \end{aligned} \tag{8}$$

$$\begin{aligned} \ddot{u}_C &= 2\dot{\vartheta}\sin\varphi\left(\dot{w}_0 + y\cos(\theta_x)\,\dot{\theta}_x - z\sin(\theta_x)\,\dot{\theta}_x\right) - \\ &\quad -2\dot{\vartheta}\cos\varphi\left(\dot{v}_0 - y\sin(\theta_x)\,\dot{\theta}_x - z\cos(\theta_x)\,\dot{\theta}_x\right) \\ \ddot{v}_C &= 2\dot{\vartheta}\cos\varphi\left(\dot{u}_0 - y\,\dot{\phi}_z + z\,\dot{\phi}_y + \psi\frac{\partial \dot{\theta}_x}{\partial x}\right) \\ \ddot{w}_C &= -2\dot{\vartheta}\sin\varphi\left(\dot{u}_0 - y\,\dot{\phi}_z + z\,\dot{\phi}_y + \psi\frac{\partial \dot{\theta}_x}{\partial x}\right) \end{aligned} \tag{9}$$

$$\begin{aligned} \ddot{u}_T &= -\dot{\vartheta}^2\left(R + x + u_0 - y\,\phi_z + z\,\phi_y + \psi\frac{\partial \theta_x}{\partial x}\right) \\ \ddot{v}_T &= \dot{\vartheta}^2\sin\varphi\cos\varphi\left(w_0 + y\sin(\theta_x) + z\cos(\theta_x)\right) - \\ &\quad -\dot{\vartheta}^2\cos\varphi^2\left(v_0 + y\;\cos(\theta_x) - z\sin(\theta_x)\right) \\ \ddot{w}_T &= -\dot{\vartheta}(t)^2\sin\varphi^2\left(w_0 + y\sin(\theta_x) + z\cos(\theta_x)\right) + \\ &\quad +\dot{\vartheta}(t)^2\sin\varphi\cos\varphi\left(v_0 + y\;\cos(\theta_x) - z\sin(\theta_x)\right) \end{aligned} \tag{10}$$

The expression of the virtual work of internal forces remains equal to the one derived for non-rotating beams, i.e. the strains are expressed by Green's strain tensor, neglecting the longitudinal displacements of second order, and the stresses are related to the strains by the Hooke's law. The stresses, the strains and the absolute acceleration are functions of the displacement components u, v and w and their derivatives, which are expressed by the displace-

ments on the reference line and the rotations of the cross sections about the reference line. The displacements on the reference line and the rotations of the cross sections are expressed by shape functions and generalized coordinates:

$$\begin{Bmatrix} u_0(\xi,t) \\ v_0(\xi,t) \\ w_0(\xi,t) \\ \theta_x(\xi,t) \\ \phi_y(\xi,t) \\ \phi_z(\xi,t) \end{Bmatrix} = \begin{bmatrix} \mathbf{N^u}(\xi)^{\mathrm{T}} & \mathbf{0} & \mathbf{0} & \mathbf{0} & \mathbf{0} & \mathbf{0} \\ \mathbf{0} & \mathbf{N^v}(\xi)^{\mathrm{T}} & \mathbf{0} & \mathbf{0} & \mathbf{0} & \mathbf{0} \\ \mathbf{0} & \mathbf{0} & \mathbf{N^w}(\xi)^{\mathrm{T}} & \mathbf{0} & \mathbf{0} & \mathbf{0} \\ \mathbf{0} & \mathbf{0} & \mathbf{0} & \mathbf{N^{\theta_x}}(\xi)^{\mathrm{T}} & \mathbf{0} & \mathbf{0} \\ \mathbf{0} & \mathbf{0} & \mathbf{0} & \mathbf{0} & \mathbf{N^{\phi_y}}(\xi)^{\mathrm{T}} & \mathbf{0} \\ \mathbf{0} & \mathbf{0} & \mathbf{0} & \mathbf{0} & \mathbf{0} & \mathbf{N^{\phi_z}}(\xi)^{\mathrm{T}} \end{bmatrix} \begin{Bmatrix} \mathbf{q_u}(t) \\ \mathbf{q_v}(t) \\ \mathbf{q_w}(t) \\ \mathbf{q_{\theta_x}}(t) \\ \mathbf{q_{\phi_y}}(t) \\ \mathbf{q_{\phi_z}}(t) \end{Bmatrix} \tag{11}$$

where $\xi \in$ [-1..1] is the local coordinate.

The shape functions used in the previous works [10, 11] are used here. The equation of motion is derived by the principle of virtual work, it is obtained in the following form:

$$\mathbf{M}\,\ddot{\mathbf{q}} + \beta\,\mathbf{KL}\,\dot{\mathbf{q}} + \mathbf{CR}\left(\mathbf{q},\dot{\vartheta}\right)\dot{\mathbf{q}} + \mathbf{KL}\,\mathbf{q} + \mathbf{KNL}(\mathbf{q})\,\mathbf{q} + \mathbf{T}\left(\mathbf{q},\dot{\vartheta}\right)\mathbf{q} = \mathbf{F} - \mathbf{R}\left(\dot{\vartheta}\right) \tag{12}$$

where $\mathbf{M}$ is the mass matrix due to relative acceleration; matrix $\mathbf{CR}\left(\mathbf{q},\dot{\vartheta}\right)$ is a consequence of Coriolis acceleration, it depends on the vector of generalized displacements, hence introduces a nonlinearity in the system, and linearly on the speed of rotation; $\mathbf{T}\left(\mathbf{q},\dot{\vartheta}\right)$ is a matrix due to the transport acceleration, it depends linearly on the relative displacement $\mathbf{q}$ (also adding non-linear terms) and quadratically on the angular speed; $\mathbf{R}$ is a vector that is a consequence of the transport acceleration, it depends quadratically on the angular speed, and it is related with the centrifugal forces that act on the beam due to the rotation. Two matrices represent the effect of elastic forces: $\mathbf{KL}$ is a stiffness matrix with constant terms and $\mathbf{KNL}$ is a stiffness matrix that depends linearly and quadratically on the vector of generalized displacements. $\mathbf{F}$ is the vector of generalized external forces. Harmonic external excitations, with the excitation frequency represented by ω are considered. Stiffness proportional damping is added to the equation of motion which depends on the damping factor β. The mass and the stiffness matrices were presented in [10], the matrices related with the rotation of the beam were presented in [11], for the cases of beams without considering setting angle and hub radios. For the current model, the setting angle appears in the matrices $\mathbf{T}\left(\mathbf{q},\dot{\vartheta}\right)$ and $\mathbf{CR}\left(\mathbf{q},\dot{\vartheta}\right)$ and the hub radios in the vector $\mathbf{R}\left(\dot{\vartheta}\right)$, they are given in the Appendix.

2.2 Cross sectional modeling

The cross section is assumed to be arbitrary with linearly varying thickness along the longitudinal axis. The cross sectional properties, such as the warping constant, the cross sectional area, the second moment of inertia are constant, for the cases of beams with constant thickness and/or width and can be calculated independently of the derivation of the equation of motion. For beams with variable thickness and/or width, the cross sectional properties are not constants, they depend on the longitudinal axis, thus they are expressed as functions of the longitudinal axis. The equation of motion is derived by integrating over the length of the beam, but including the cross sectional properties in the integration.

The warping function is obtained numerically by solving the Laplace equation with Neumann boundary conditions [15]:

$$\begin{aligned} \nabla^2\psi &= 0 \quad \text{in } \Omega \\ \frac{\partial\psi}{\partial n} &= z\,n_y - y\,n_z \quad \text{on } \Gamma \end{aligned} \tag{13}$$

where Ω denotes the cross section and Γ is the contour of the cross section. Equation (13) is solved by finite element method, as a result the warping and the torsional constants are obtained using Gauss integration points.

The linearly varying thickness of the beam is taken into account by expressing all cross sectional properties as functions of the local coordinate ξ. Let $f(\xi)$ be a linear function which defines the thickness of the beam as a function of the local longitudinal coordinate ξ. The cross sectional properties are express by their values on the left side of the beam, i.e. at ξ = -1, and the function $f(\xi)$. For example, the area of the beam $A(\xi)$, which has dimension m^2 and the warping constant $C_w(\xi)$, which has dimension m^6 are expressed as:

$$A(\xi) = A\left(\frac{f(\xi)}{f(-1)}\right)^2$$
$$C_w(\xi) = C_w\left(\frac{f(\xi)}{f(-1)}\right)^6 \tag{14}$$

where A and C_w are the cross sectional area and the warping constant at the left side of the beam, ξ = -1. The expressions $A(\xi)$, $C_w(\xi)$ plus the additional cross sectional properties are used for the derivation of the equation of motion. As an example, the bending matrix $\mathbf{K1}_{33}$, defined in [10] for constant cross sections, is obtained here on the following way:

$$\mathbf{K1_{33}} = \lambda G \int_V \frac{d\boldsymbol{N^w}}{dx}\frac{d\boldsymbol{N^{wT}}}{dx} dV = \lambda G \frac{2}{l}\int_{-1}^{1} A(\xi)\frac{d\boldsymbol{N^w}}{d\xi}\frac{d\boldsymbol{N^{wT}}}{d\xi} d\xi \tag{15}$$

where λ is the shear correction factor, l is the length of the beam and G is the shear modulus. The rest of the matrices are obtained on similar way.

3 VALIDATION

The proposed model for tapered beams with arbitrary cross sections is first validated by generating a fine mesh of three-dimensional elements. The natural frequencies and the static deformations are compared. A thin-walled beam with rectangular cross section is used. The length of the beam is chosen to be 0.58 m, the left side is with dimensions 0.02 x 0.015 m and thickness 0.001 m and the right side is with dimensions 0.01 x 0.0075 m and thickness 0.0005 m. The material properties are (aluminium): $E = 7.0^{10}\ N/m^2$, $\rho = 2778\ kg/m^3$, $\nu = 0.34$. The beam is with clamped-free boundary conditions. The beam model presented at the previous section, is derived using 10 shape functions for each displacement, i.e. 60 DOF.

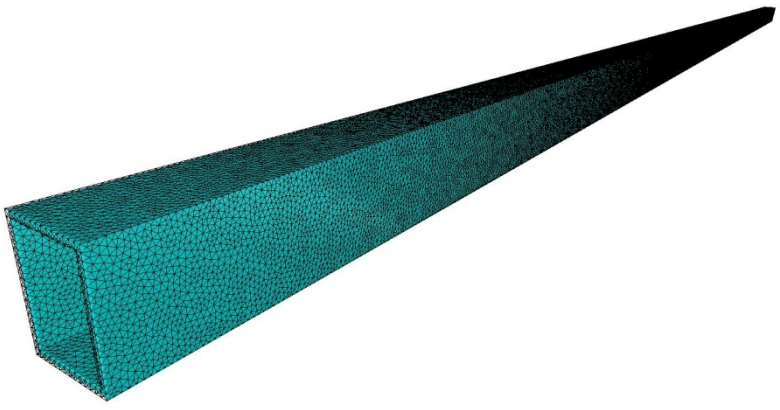

Figure 2. Three-dimensional beam structure used for validation of the proposed model.

The FEM software Elmer [16], which is suitable for large deformation problems, is used to validate the thin-walled beam. A fine mesh of quadratic tetrahedrons is generated using Gmsh

[17]. The mesh has 235914 elements which results into 462725 nodes, each node has three DOF, i.e. the resulting system has more than 1 million DOF. It is solved by parallel computing, using the library Mumps (MUltifrontal Massively Parallel Solver) [18] which is a parallel direct sparse solver. The generated three-dimensional beam is shown on Figure 2. It was verified, by reducing the edges of the tetrahedrons by two, that the results obtained by the large-scale model are converged.

In Table 1 are presented the natural frequencies from the derived beam model and from the three-dimensional software Elmer. Even though the beam is tapered, the cross section remains symmetric with respect to the transverse axes, thus the bending and the torsional modes remain uncoupled.

For further validation of the model, static deformation due to static forces are compared of both models, considering geometrical type of nonlinearity. Uniformly distributed forces are applied along the beam sides in both transverse and longitudinal directions. The results are summarized in Table 2.

The results from both tables confirm that the implemented model for thin-walled tapered beams gives very close results to the same beam structure modeled with three-dimensional finite elements. This beam model, including the rotational terms will be used in the next section. One should note that the beam model is not suitable for large rotations of the cross section, thus the numerical experiments will be limited within the displacements presented and validated in Table 2.

Mode	Beam model	Elmer	Mode shape	Difference %
1	409.65	409.78	Bending xz	0.032
2	514.74	514.97	Bending xy	0.045
3	1725.87	1720.67	Bending xz	0.302
4	2164.70	2160.70	Bending xy	0.185
5	4266.60	4229.38	Bending xz	0.880
6	5335.58	5304.70	Bending xy	0.582
7	8004.81	7869.62	Bending xz	1.718
8	9969.86	9857.35	Bending xy	1.141
9	11449.33	11447.27	Torsion	0.018
10	12913.34	12549.35	Bending xz	2.900

Table 1: First 10 natural frequencies (rad/s) of thin-walled tapered cantilever beam, comparison of the beam model with Elmer.

Total force [N]	Beam model		Elmer model		Difference %	
(F_u, F_v, F_w)	v	w	v	w	v	w
(0, 0, 500)	0.0	0.104911	0.0	0.102897	-	1.92
(0, 500, 500)	0.066618	0.105105	0.065180	0.102138	2.16	2.82
(100, 0, 500)	0.0	0.089321	0.0	0.088223	-	1.23
(100, 500, 500)	0.059885	0.089431	0.058982	0.087738	1.51	1.89
(200, 0, 500)	0.0	0.078108	0.0	0.077448	-	0.84
(200, 500, 500)	0.054517	0.078176	0.053776	0.077114	1.36	1.36

Table 2: Comparison of static deformation (meters) on the free end of the cantilever beam, the applied force is uniformly distributed along the beam's sides, v – transverse displacement in y direction, w – transverse displacement in z direction.

4 NUMERICAL RESULTS

In this section the numerical results of the thin-walled tapered beam rotating at constant speed are presented. First, the influence of the setting angle and the speed of rotation of the natural frequencies and mode shapes is discussed and then the nonlinear forced vibrations at time domain are presented.

4.1 Free vibrations of rotating beams

It is well known that the speed of rotation makes the beam stiffer and increases the natural frequencies [1-3], as well that the hub radios increases the natural frequencies of rotating beams. In this subsection, special attention is given to the influence of the setting angle on the natural frequencies. On Figure 3 is presented the variation of the first and second natural frequencies with the speed of rotation and the setting angle.

It should be pointed out that the transverse displacements v_0 and w_0 couple in the linear modes of rotating beams when the setting angle is different from zero or $k\pi/2\,, k \in \mathbb{Z}$ (even though the cross section is symmetric). The coupling comes from the transport acceleration, i.e. from sub-matrices $\mathbf{T}_{23}$ and $\mathbf{T}_{32}$, which are non-zero if the setting angle is different from $k\pi/2\,, k \in \mathbb{Z}$. On Figure 4 are presented the transverse components of the first linear mode of rotating beam with angular velocity $\dot{\vartheta} = 100$ rad/s, for different setting angles. For value of the setting angle $\varphi = 0$ rad or $\varphi = 2\pi$ rad, only the component of w_0 is excited and the vibration is perpendicular to the plane of rotations. i.e. the mode is flapwise. For setting angel $\varphi = \pi$ rad, also only the component of w_0 is excited, but now it vibrates in the plane parallel to the plane of rotation i.e. it is lagwise mode. For all other values of the setting angel φ, both components of the transverse displacements v_0 and w_0 are excited and the vibration is not fixed in a plane parallel or perpendicular to the plane of rotation.

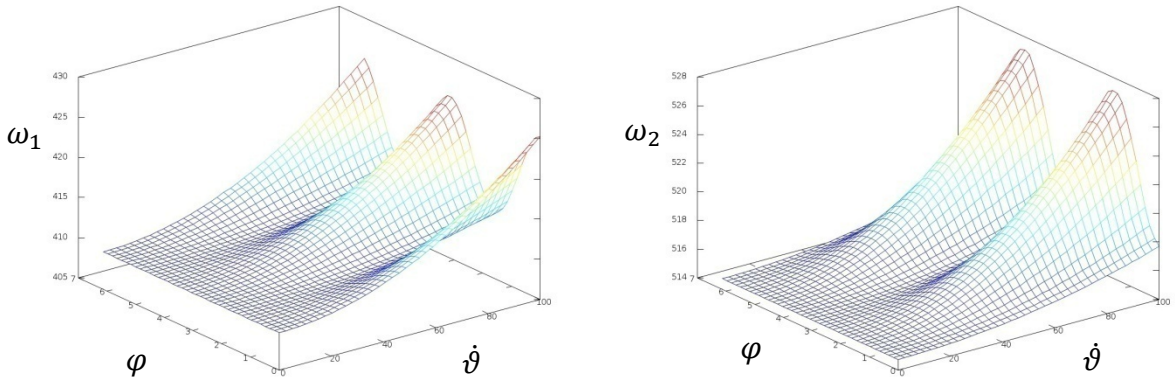

(a) (b)

Figure 3. Variation of the (a) first and (b) second natural frequency with the speed of rotation and setting angle.

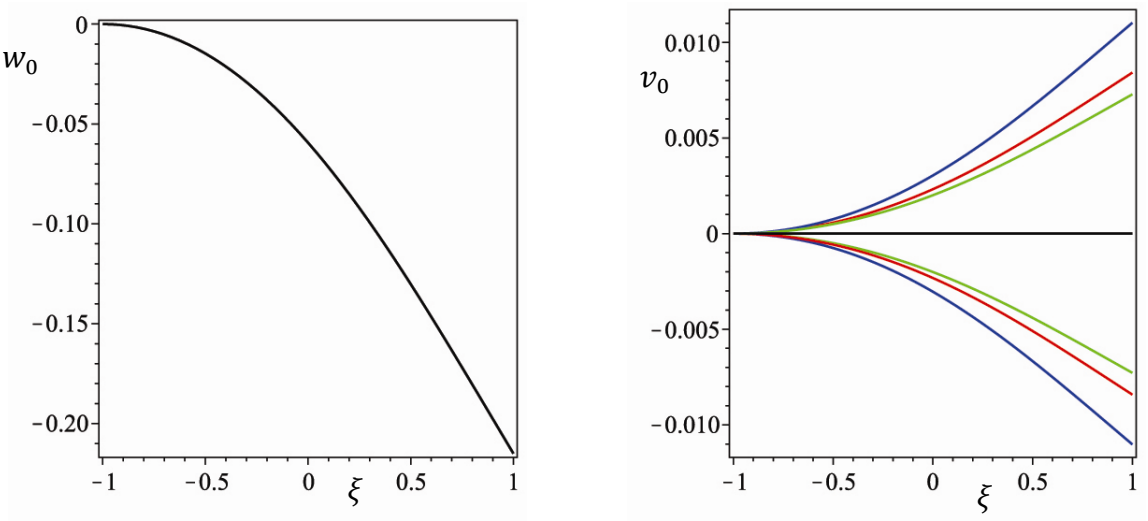

(a) (b)

Figure 4. Linear mode shapes of the beam rotating at angular speed 100 rad/s for various setting angles, (a) component of transverse displacement w_0, (b) component of transverse displacement v_0, — $\varphi = 0, \pi/2, \pi$; — $\varphi = \pm\pi/8$, — $\varphi = \pm\pi/4$, — $\varphi = \pm 3\pi/8$, negative setting angle results into component of transverse displacement v_0 with negative amplitude.

4.2 Forced vibrations of rotating beams

Forced vibrations in time domain due to harmonic excitations are presented and investigated in this section for beams rotating with constant speed $\dot{\vartheta} = 100$ rad/s. An external force with amplitude 50 000 N and excitation frequency 425.25 rad/s is applied in Z direction of the fixed coordinate system, i.e. the force is perpendicular to the plane of rotation. A damping proportional to the linear stiffness matrix with $\beta = 0.0001$ is considered. The steady-state responses of the transverse displacements of the beam are presented for different setting angles.

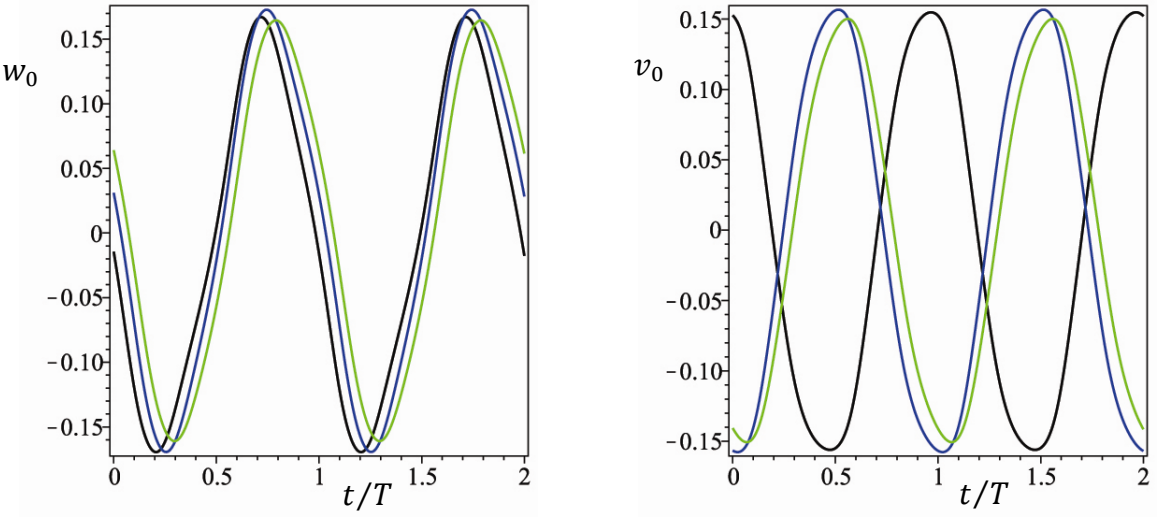

(a) (b)

Figure 5. Steady-state forced responses of the transverse displacements of the beam on the free end due to external force $F_Z = 50000\cos(425.25\,t)$, — $\varphi = 0$, — $\varphi = \pi/8$, — $\varphi = \pi/4$, $\dot{\vartheta} = 100$ rad/s, t – time, T – period of vibration.

On Figure 5, are shown the forced responses of the beam for three different setting angles: 0, $\pi/8$ and $\pi/4$. It is noted that with changes of the setting angle, the force remains in the

same direction (perpendicular to the plane of rotation), and changes of the setting angle spread the external force in y and z directions in the transport coordinate system. It can be seen that for the three different setting angles, the amplitudes of vibration change slightly. Also, in the case of zero setting angle, $\varphi = 0$, i.e. when the transverse force is applied only in z direction of the beam, the transverse displacement v_0 is excited with amplitude similar to the transverse displacement w_0. One could expect that for that case, $\varphi = 0$, the transverse displacement v_0 will be excited due to acceleration of Coriolis and it will vibrate with smaller amplitude in comparison to w_0. Nevertheless, Figure 5 shows that the response amplitude of v_0 is similar to the amplitude of w_0.

Further, to investigate the influence of the acceleration of Coriolis, the responses at time domain of the same example, $\varphi = 0$, but without Coriolis forces, were obtained and shown in Figure 6. The difference between the responses of the models with and without Coriolis forces is significant (Figure 6 (a)), it is also verified that the transverse displacement v_0 is not excited, in the absence of Coriolis forces. It is concluded that the big amplitudes of the transverse displacement v_0, on Figure 5 (b) are related with loose of stability of the beam, due to interaction of both transverse modes. Even though when the external force is applied only in z direction (in the case $\varphi = 0$), the transverse displacement v_0 is excited, if there is small disturbance (Figure 6 (b)). This phenomenon is due to symmetry-breaking bifurcation point, similar bifurcation point, but for clamped-clamped beams was presented in [19]. In Figure 5, the small excitation of v_0 comes from the Coriolis forces. Thus, the solution obtained when the acceleration of Coriolis is neglected on Figure 6 (a), corresponds to the unstable solution, which presents vibration in one plane (v_0 is not excited). An unstable solution is obtained with time integration method, such as Newmark, because v_0 is not excited and there is no coupling between both transverse displacements, and the problem to solve is two dimensional, where the symmetry-breaking bifurcation point does not exists. It was also verified that, for the current case, the Coriolis forces slightly change the response –Figure 6 (b). The significant difference of the phase of the transverse displacement v_0 for $\varphi = 0$, in comparison with the rest cases of the setting angle (Figure 5 (b)), is explained by the two stable branches which arise from the symmetry-breaking bifurcation point.

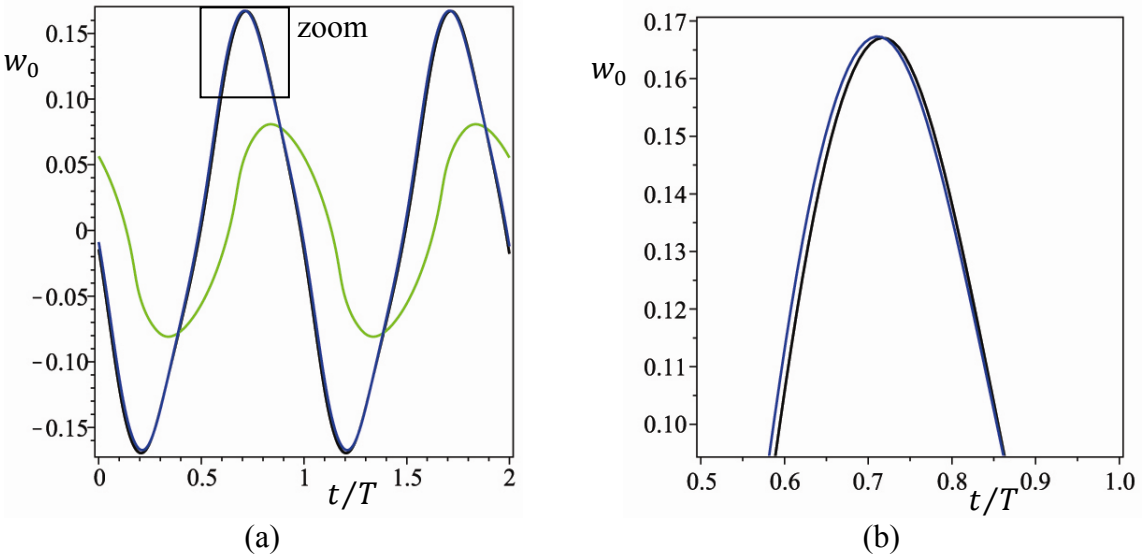

Figure 6. (a) Steady-state forced responses of the transverse displacement w_0 of the beam on the free end due to external force $F_Z = 50000\cos(425.25\,t)$, $\varphi = 0$, $\dot{\vartheta} = 100$ rad/s, — with Coriolis forces, — without Coriolis forces, — without Coriolis forces, but with initial disturbance of v_0, (b) zoom of (a), t – time, T – period of vibration.

Finally, a discussion about the equality of the amplitudes of vibration for the different setting angles is presented. One could expect that increasing the setting angle will decrease the amplitude of w_0 and will increase the amplitude of v_0, because the external force is decreased in z direction and it is increased in y direction (for $0 \leq \varphi \leq \pi/2$). However, the amplitudes remain similar. It is because of the nonlinear terms and the fact the excitation frequency remains the same, i.e. in nonlinear vibrations the amplitude depends on the frequency of vibration [20]. This is not true for linear vibrations and the influence of the setting angle on the amplitude of vibration can be seen on Figure 7.

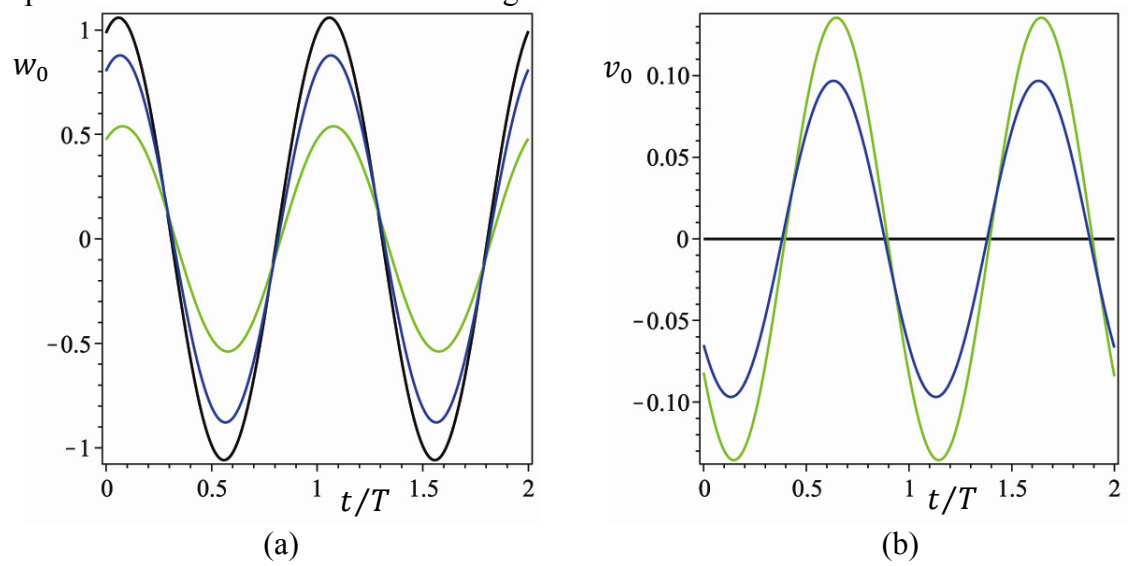

(a) (b)

Figure 7. (a) Steady-state forced responses of the transverse displacements w_0 and v_0 of the linear beam model on the free end due to external force $F_Z = 50000\cos(425.25\,t)$, $\dot{\vartheta} = 100$ rad/s, ━ $\varphi = 0$, ━ $\varphi = \pi/8$, ━ $\varphi = \pi/4$, t – time, T – period of vibration.

5 CONCLUSION

Nonlinear vibrations of rotating beams due to harmonic excitations were investigated. First a model of 3D beams rotating at constant speed about a fixed axis was presented, a setting angle and hub radios ware included in the model. The equation of motion was derived in the rotating coordinate system, and the rotation was taken into account by the inertia forces. Then, it was shown how the cross section was modeled and the tapered ratio considered in the equation of motion.

The beam model was validated by generating an equivalent beam structure with three-dimensional finite elements. The natural frequencies and the static deformations, of non-rotating beam, were compared and it was demonstrated that the reduced model gives results in agreement with the large-scale model. It should be outlined, that the reduced model is suitable for problems where the cross section does not change in its own plane and the rotations of the cross section about the transverse axes are moderate.

Thin-walled box beams with linearly varying thickness and width were investigated. The influence of the speed of rotation and the setting angle on the natural frequencies was presented. It was shown that in linear free vibrations, both transverse displacements are coupled, for values of the setting angle different from zero, due to the inertia forces, which result from the rotation.

Nonlinear forced steady-state responses were examined for different setting angles. The amplitude of vibration changes slightly with the setting angle, due to the geometrical nonlinear terms, while in linear models this change is significant. Steady-state responses which

correspond to the stable branches which arise from symmetry-breaking bifurcation point were obtained and presented.

ACKNOWLEDGEMENT

The research work carried out in the paper is supported by the project AComIn "Advanced Computing for Innovation", grant 316087, funded by the FP7 Capacity Programme (Research Potential of Convergence Regions) and Bulgarian NSF Grant DCVP 02/1.

APPENDIX

In this appendix the matrices and vectors that result from the transport acceleration and acceleration of Coriolis are presented. The transport acceleration results in the following matrix and vector:

$$\mathbf{T}(\mathbf{q},\dot{\vartheta}) = \begin{bmatrix} \mathbf{T_{11}} & \mathbf{0} & \mathbf{0} & \mathbf{0} & \mathbf{0} & \mathbf{0} \\ \mathbf{0} & \mathbf{T_{22}} & \mathbf{T_{23}} & \mathbf{0} & \mathbf{0} & \mathbf{0} \\ \mathbf{0} & \mathbf{T_{32}} & \mathbf{T_{33}} & \mathbf{0} & \mathbf{0} & \mathbf{0} \\ \mathbf{0} & \mathbf{0} & \mathbf{0} & \mathbf{T_{44}} & \mathbf{0} & \mathbf{0} \\ \mathbf{0} & \mathbf{0} & \mathbf{0} & \mathbf{0} & \mathbf{T_{55}} & \mathbf{0} \\ \mathbf{0} & \mathbf{0} & \mathbf{0} & \mathbf{0} & \mathbf{0} & \mathbf{T_{66}} \end{bmatrix}$$

$$\mathbf{R}(\dot{\vartheta}) = \begin{Bmatrix} \mathbf{R_1} \\ \mathbf{0} \\ \mathbf{0} \\ \mathbf{R_4} \\ \mathbf{0} \\ \mathbf{0} \end{Bmatrix}$$

where

$$\mathbf{T_{11}} = -\dot{\vartheta}(t)^2\,\rho \int_V \mathbf{N^u}^{\mathrm{T}}\,\mathbf{N^u}\,dV$$

$$\mathbf{T_{22}} = -\dot{\vartheta}(t)^2\,\rho\,\cos\varphi^2 \int_V \mathbf{N^v}^{\mathrm{T}}\,\mathbf{N^v}\,dV$$

$$\mathbf{T_{23}} = \dot{\vartheta}(t)^2\,\rho\,\cos\varphi\sin\varphi \int_V \mathbf{N^v}^{\mathrm{T}}\,\mathbf{N^w}\,dV$$

$$\mathbf{T_{32}} = \dot{\vartheta}(t)^2\,\rho\,\cos\varphi\sin\varphi \int_V \mathbf{N^w}^{\mathrm{T}}\,\mathbf{N^v}\,dV$$

$$\mathbf{T_{33}} = -\dot{\vartheta}(t)^2\,\rho\,\sin\varphi^2 \int_V \mathbf{N^w}^{\mathrm{T}}\,\mathbf{N^w}\,dV$$

$$\mathbf{T_{44}} = \dot{\vartheta}(t)^2\,\rho\,(\cos\varphi^2 - \sin\varphi^2) \int_V (y^2 - z^2)\,\mathbf{N^{\theta_x}}^{\mathrm{T}}\,\mathbf{N^{\theta_x}}dV +$$

$$+\dot{\vartheta}(t)^2\,\rho\,\cos\varphi\sin\varphi \int_V (z^2 - y^2)\,\mathbf{N^{\theta_x}}^{\mathrm{T}}\,\mathbf{N^{\theta_x}}\,\theta_x\,dV - \dot{\vartheta}(t)^2\,\rho \int_V \psi^2 \frac{\mathrm{d}\mathbf{N^{\theta_x}}^{\mathrm{T}}}{\mathrm{d}x}\frac{\mathrm{d}\mathbf{N^{\theta_x}}}{\mathrm{d}x}dV$$

$$\mathbf{T_{55}} = -\dot{\vartheta}(t)^2\,\rho \int\limits_V z^2\,\mathbf{N^{\phi_y}}^{\mathrm{T}}\mathbf{N^{\phi_y}}\,dV$$

$$\mathbf{T_{66}} = -\dot{\vartheta}(t)^2\,\rho \int\limits_V y^2\,\mathbf{N^{\phi_z}}^{\mathrm{T}}\mathbf{N^{\phi_z}}\,dV$$

$$\mathbf{R_1} = \dot{\vartheta}(t)^2\,\rho \int\limits_V (R+x)\,\mathbf{N^{u}}^{\mathrm{T}}\,dV$$

$$\mathbf{R_4} = \dot{\vartheta}(t)^2\,\rho\,\cos\varphi\sin\varphi \int\limits_V (-y^2+z^2)\,\mathbf{N^{\theta_x}}^{\mathrm{T}}\,dV$$

The acceleration of Coriolis results in the following matrix:

$$\mathbf{CR}(\mathbf{q},\dot{\vartheta}) = \begin{bmatrix} \mathbf{0} & \mathbf{CR_{12}} & \mathbf{CR_{13}} & \mathbf{0} & \mathbf{0} & \mathbf{0} \\ \mathbf{CR_{21}} & \mathbf{0} & \mathbf{0} & \mathbf{0} & \mathbf{0} & \mathbf{0} \\ \mathbf{CR_{31}} & \mathbf{0} & \mathbf{0} & \mathbf{0} & \mathbf{0} & \mathbf{0} \\ \mathbf{0} & \mathbf{0} & \mathbf{0} & \mathbf{0} & \mathbf{CR_{45}} & \mathbf{CR_{46}} \\ \mathbf{0} & \mathbf{0} & \mathbf{0} & \mathbf{CR_{54}} & \mathbf{0} & \mathbf{0} \\ \mathbf{0} & \mathbf{0} & \mathbf{0} & \mathbf{CR_{64}} & \mathbf{0} & \mathbf{0} \end{bmatrix}$$

where

$$\mathbf{CR_{12}} = -2\,\dot{\vartheta}(t)\,\rho\cos\varphi \int\limits_V \mathbf{N^{u}}^{\mathrm{T}}\,\mathbf{N^{v}}\,dV$$

$$\mathbf{CR_{13}} = 2\,\dot{\vartheta}(t)\,\rho\sin\varphi \int\limits_V \mathbf{N^{u}}^{\mathrm{T}}\,\mathbf{N^{w}}\,dV$$

$$\mathbf{CR_{21}} = 2\,\dot{\vartheta}(t)\,\rho\cos\varphi \int\limits_V \mathbf{N^{v}}^{\mathrm{T}}\,\mathbf{N^{u}}\,dV$$

$$\mathbf{CR_{31}} = -2\,\dot{\vartheta}(t)\,\rho\sin\varphi \int\limits_V \mathbf{N^{w}}^{\mathrm{T}}\,\mathbf{N^{u}}\,dV$$

$$\mathbf{CR_{45}} = -2\,\dot{\vartheta}(t)\,\rho\cos\varphi \int\limits_V z^2\;\mathbf{N^{\theta_x}}^{\mathrm{T}}\,\mathbf{N^{\phi_y}}\,dV + 2\,\dot{\vartheta}(t)\,\rho\sin\varphi \int\limits_V z^2\;\mathbf{N^{\theta_x}}^{\mathrm{T}}\,\mathbf{N^{\phi_y}}\,\theta_x\,dV$$

$$\mathbf{CR_{46}} = 2\,\dot{\vartheta}(t)\,\rho\sin\varphi \int\limits_V y^2\;\mathbf{N^{\theta_x}}^{\mathrm{T}}\,\mathbf{N^{\phi_z}}\,dV + 2\,\dot{\vartheta}(t)\,\rho\cos\varphi \int\limits_V y^2\;\mathbf{N^{\theta_x}}^{\mathrm{T}}\,\mathbf{N^{\phi_z}}\,\theta_x\,dV$$

$$\mathbf{CR_{54}} = 2\,\dot{\vartheta}(t)\,\rho\cos\varphi \int\limits_V z^2\,\mathbf{N^{\phi_y}}^{\mathrm{T}}\,\mathbf{N^{\theta_x}}\,dV - 2\,\dot{\vartheta}(t)\,\rho\sin\varphi \int\limits_V z^2\,\mathbf{N^{\phi_y}}^{\mathrm{T}}\,\mathbf{N^{\theta_x}}\,\theta_x\,dV$$

$$\mathbf{CR_{64}} = -2\,\dot{\vartheta}(t)\,\rho\sin\varphi \int\limits_V y^2\,\mathbf{N^{\phi_z}}^{\mathrm{T}}\,\mathbf{N^{\theta_x}}\,dV - 2\,\dot{\vartheta}(t)\,\rho\cos\varphi \int\limits_V y^2\,\mathbf{N^{\phi_z}}^{\mathrm{T}}\;\mathbf{N^{\theta_x}}\,\theta_x\,dV$$

REFERENCES

[1] D. Hodges, M. Rutkowski, Free vibration analysis of rotating beams by a variable-order finite-element method. *AIAA Journal*, 19, 1459-1466, 1981.

[2] T. Yokoyama, Free vibration characteristics of rotating Timoshenko beams. *International Journal of Mechanical Sciences*, 30, 743-755, 1988.

[3] A. Bazoune, Y. Khulief, N. Stephen, Further results for modal characteristics of rotating tapered Timoshenko beams. Journal *of Sound and Vibration*, 219, 157-174, 1999.

[4] S. Lin, K. Hsiao, Vibration analysis of a rotating Timoshenko beam. *Journal of Sound and Vibration*, 240, 303-322, 2001.

[5] H. Yoo, S. Shin, Vibration analysis or rotating cantilever beams. *Journal of Sound and Vibration*, 212, 807-828, 1998.

[6] E. Pesheck, C. Pierre, S. Shaw, Modal reduction of a nonlinear rotating beam through nonlinear normal modes. *Journal of Vibration and Acoustics*, 124, 229-236, 2002.

[7] Ö. Turhan, G. Bulut, On nonlinear vibrations of a rotating beam. *Journal of Sound and Vibration*, 322, 314-335, 2009.

[8] D. Younesian, E. Esmailzadeh, Non-linear vibration of variable speed rotating viscoelastic beams. *Nonlinear Dynamics*, 60, 193-205, 2010.

[9] F.M. Jensen, P.H. Nielsen, A. Roczek-Sieradzan, T. Sieradzan, K. Branner, R. Bitsche, On innovative concepts of wind turbine blade design. *European Wind Energy Conference and Exhibition 2011, EWCE 2011*, 275-279, 2011.

[10] S. Stoykov, P. Ribeiro, Vibration analysis of rotating 3D beams by the p-version finite element method. *Finite Elements in Analysis and Design*, 65, 76-88, 2013.

[11] S. Stoykov, P. Ribeiro, Nonlinear forced vibrations and static deformations of 3D beams with rectangular cross section: The influence of warping, shear deformation and longitudinal displacements. *International Journal of Mechanical Sciences*, 52, 1505-1521, 2010.

[12] C. Wang, J. Reddy, K. Lee, *Shear deformable beams and plates*, Elsevier, Oxford, 2000.

[13] G. Wempner, D. Talaslidis, *Mechanics of solids and shells. Theory and Application*, CRC Press, Boca Raton, Florida, 2003.

[14] A.A. Shabana, *Dynamics of multibody systems*, Cambridge University Press, 2005.

[15] I. Sokolnikoff, *Mathematical theory of elasticity*, McGraw-Hill, 1956.

[16] Elmer web site: www.csc.fi/elmer (last time visited 15/02/2013).

[17] C. Geuzaine and J.-F. Remacle, Gmsh: a three-dimensional finite element mesh generator with built-in pre- and post-processing facilities. *International Journal for Numerical Methods in Engineering*, 79, 1309-1331, 2009.

[18] P. R. Amestoy, A. Guermouche, J. Y. L'Excellent, S. Pralet, Hybrid scheduling for the parallel solution of linear systems. *Parallel Computing*, 32, 136-156, 2006.

[19] S. Stoykov, P. Ribeiro, Stability of nonlinear periodic vibrations of 3D beams. *Nonlinear Dynamics*, 66, 335-353, 2011.

[20] G. Kerschen, M. Peeters, J. C. Golinval, A. Vakakis, Nonlinear normal modes, Part I: A useful framework for the structural dynamicist. *Mechanical Systems and Signal Processing*, 23, 170-194, 2009.